Available online at www.sciencedirect.com
SCIENCE DIRECT®
Polymer 45 (2004) 1867–1877
polymer
www.elsevier.com/locate/polymer

Polymerization of a thermoset system into a thermoplastic matrix. Effect of the shear

Laure Meynie, Françoise Fenouillot*, Jean-Pierre Pascault

Laboratoire des Matériaux Macromoléculaires, UMR-CNRS 5627, Institut National des Sciences Appliquées, 17 Avenue Jean Capelle, 69 621 Villeurbanne Cedex. France

Received 7 April 2003; received in revised form 15 November 2003; accepted 17 December 2003

Abstract

This study concerns the morphology development of a blend based on a thermoplastic matrix with a reactive system undergoing polymerization. The system consists of 60 weight percent of polystyrene and 40 weight percent of a thermoset precursor with a low reactivity diamine (4,4′-methylenebis(2,6-diethylaniline)). Experiments were carried out in a temperature controlled oil bath and in an internal mixer. In the first case, the reaction induced phase separation process was conducted under quiescent conditions and, in the second case, under dynamic conditions. Although the kinetic study showed no noticeable difference between the static and dynamic experiments, the final morphologies obtained are quite different depending on shear. Whereas spherical particles (~ 3 μm) are obtained under static conditions, irregular particles and larger dimensions characterize the morphology under shear. The classical phenomenon of droplet break up/coalescence is not applicable when an insoluble fraction is present. In the vicinity of the gelation time, the particles tend to aglomerate in an irreversible way and so the process of shape relaxation leading to spherical particles becomes impossible.

Keywords: Thermoplastic–thermoset blend; Morphology; Shear

1. Introduction

Thermoplastic (TP)/thermoset (TS) blends are materials resulting from the mixing of a thermoplastic polymer with thermoset precursors. Most often, the phase diagram of the thermoplastic/precursors system shows an upper-critical-solution temperature (UCST), i.e. the miscibility increases with increasing temperature [1].

At the beginning of the polymerization at constant temperature T_i, the system with composition $\phi_{TP(0)}$ is homogeneous (Fig. 1). As the reaction proceeds, the system becomes less miscible due to the increasing length of the growing chains, to the increasing degree of crosslinking or by changes in components interactions. At a certain conversion x, the cloud point curve passes through the initial point ($\phi_{TP(0)}$, T_i). An increase in conversion from this value makes the system metastable, and phase separation may begin to take place.

The location of $\phi_{TP(0)}$ with respect to the critical composition ϕ_{crit} plays a role in determining the phase separation mechanism and so, depending on the composition of the initial blend, ϕ_{M0}, several types of morphologies may be obtained. Girard-Reydet et al. [2] demonstrated that nucleation and growth occurs at off-critical composition (typically $\geq 30\%$ of TP). All small concentration fluctuations tend to decay and hence separation can proceed only by overcoming the barrier with a large fluctuation in composition. This fluctuation is called a nucleus and, once such a nucleus is formed, it grows by a normal diffusion process.

Subsequent to phase separation, the dispersed particles grow in size with time by the diffusion of the monomers. They also grow by coalescence and/or by an evaporation–condensation process (Ostwald Ripening). Obviously, the morphology of a TP/TS blend after full polymerisation of the monomers may have a strong influence on its properties. This is discussed extensively in the literature. The morphology is controlled by factors such as initial miscibility, TP concentration [3,4], processing conditions [5–7], reaction rate [8], viscosity [9–11] and interfacial

* Corresponding author. Tel.: +33-4-72-43-83-81; fax: +33-4-72-43-85-27.
E-mail address: francoise.fenouillot@insa-lyon.fr (F. Fenouillot).

0032-3861/$ - see front matter © 2004 Elsevier Ltd. All rights reserved.
doi:10.1016/j.polymer.2003.12.070

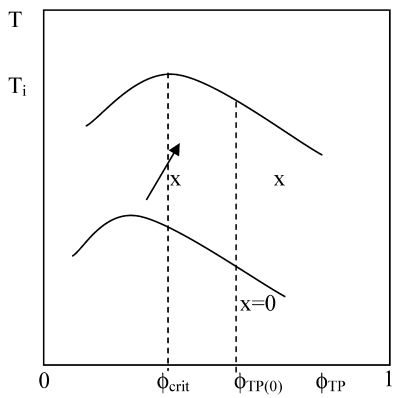

Fig. 1. Temperature versus composition transformation diagram for a thermoplastic thermoset blend with an upper critical solution temperature behavior. (— cloud-point curve).

tension [12,13]. Bonnet et al. [14] and Venderbosh et al. [15–17] obtained micron sized epoxy spheres in the thermoplastic (polyetherimide or polyphenylene ether) matrix upon curing the initially homogeneous epoxy/thermoplastic (30/70) in quiescent conditions.

Janssen et al. [18] studied the morphology of polyphenylene ether-polystyrene/epoxy blends resulting from chemically induced phase separation processes. They obtained an extremely fine, sub-micron, morphology for solutions that vitrify upon cooling by applying a protocol of curing at the glass transition temperature of the initial solution. In this case, phase separation occurs in a highly viscous medium that restricts the coarsening process. During the additional post-curing steps, necessary to reach a maximum epoxy conversion, these morphologies are maintained.

Particle coarsening due to the coalescence phenomena of dispersed phase has been studied in a number of works [19–22]. Coalescence is a process in which two particles collide and physically merge into one particle. For two particles to fuse, they must come into close proximity of each other by some flow process driven by forces such as Brownian motion. The Smoluschowski theory of coalescence [23] is based on the assumption that the rate of coalescence is determined by the approach of the particles i.e. the Brownian motion. This model is adequate only for dilute systems. For blends containing 10 or more percent of the dispersed phase, the rate of coalescence is also determined by other mechanisms such as collision induced collision [24]. In this case, the average distance of a droplet from its nearest neighbour is smaller than its radius.

Regardless of the approach mechanism, the removal of the continuous phase between two droplets is also a rate determining step, which is a function of the viscosity of the matrix and of the droplet.

Evaporation–condensation, also called the Ostwald ripening process, involves the dissolution and disappearance of the smallest dispersed particles to the benefit of large particles [25,26]. This process is driven by the tendency to decrease the total interfacial area. In fact, well-separated droplets, having well defined interfaces, will coarsen due to the fact that smaller droplets with a smaller radius of curvature have a higher solubility. Hence, the average particle size increases whereas the number of particles decreases. Mirabella et al. [27] studied the coarsening of a hydrogenated polybutadiene (HPB) and high-density polyethylene (HDPE). They found that the system coarsened according to the kinetics of the evaporation–condensation mechanism.

The above literature was concerned with blends demixing under quiescent conditions. If the blend is subjected to flow, that is shear stress, the morphology development is still driven by the phase separation process. However, additional significant effects have to be considered.

A mechanism that is obviously not encountered under quiescent situation is drop deformation and breakup. Taylor developed a theory to predict the break-up of individual droplets for Newtonian fluids [28,29]. The predicted drop size for a simple shear field is proportional to the interfacial tension and inversely proportional to the shear rate and the matrix viscosity. This theory applies to systems with vanishingly small concentrations of the dispersed phase and drop break up is predicted to occur only for systems when $\eta_d/\eta_m < 2.5$ where η_d is the viscosity of the droplets and η_m the viscosity of the matrix. It has also been shown that the particle size dependence on viscosity ratio exhibits a minimum between $\eta_d/\eta_m = 0.1$ and 1. Moreover, Grace [9] showed that extensional flow was more effective for inducing drop break up over a much wider range of viscosity ratios. For example, extruders and compounding mixers impose a mixture of both shear and elongational flows on the polymer melt.

The shear induces deformation and possibly break up of the droplet, that is size reduction. However, the presence of shear also promotes coalescence of the droplets that leads to coarsening of the morphology. The coalescence of droplets is known to occur via droplet collision followed by drainage and rupture of the film between droplets.

In simple shear flow, the ‘external flow’ and the volume fraction of the dispersed phase govern the collision frequency. In addition, the external flow is responsible for the contact force and the interaction time of collision conditioning the film drainage.

The coalescence probability P_{coa} i.e. the probability that a collision takes place within the process time available and, additionally, that this collision is successful and leads to coalescence is defined as: $P_{coa} = P_{coll} \times P_{drain}$ where P_{coll} is the collision probability and P_{drain} the probability of drainage of the liquid film between particle

P_{coll} increases with the shear rate applied and the volume fraction of the dispersed phase, whereas it is independent of the drop size. P_{drain} is more complicated as it depends on the mobility of the interface [30]. The draining becomes more difficult for immobile interfaces because friction between

the fluid film and the droplet surface increase. To ensure the drainage of the film, small deformation rates are required.

Under shear, the coalescence induced by the collision of the droplets is probably so predominant that we may simply neglect those induced by evaporation–condensation or by 'static' collisions.

The final morphology of polymer blends, when such mixtures are subjected to mechanical mixing, is a balance between break-up and coalescence phenomena.

To the best of our knowledge, no attempt has been made to model the evolution of the size of the dispersed phase of a blend in which the viscosity of both phases evolves with time, as is encountered for reaction induced phase separation processes. Nevertheless, experimental studies exist but in most of them, only the dispersed phase viscosity varies. Vivier et al. [31] studied the formation of a nodular morphology of in situ crosslinked thermoset under shear in a thermoplastic matrix. They were interested in the final morphology and hence did not follow the evolution of the morphology during curing. Whereas they obtained spherical particles of 0.7–1.4 μm diameter of bisphenol A diglycidyl ether (DGEBA)/isophorone diamine (IPD) in a polystyrene (PS) matrix under quiescent conditions, they did not manage to form a spherical structure under shear.

De Loor et al. [32] followed the development of the morphology of a reactive blend of ethylene vinyl acetate (EVA) and ethylene methyl acrylate (EMA) copolymers dispersed in a polypropylene (PP) matrix. The EVA/EMA elastomer was crosslinked in the presence of a catalyst during the melt mixing of the blend in a twin screw extruder. It appeared that the local morphology was strongly dependent on the extent of the crosslinking reaction. The authors observed a fine dispersion after the melting zone, but with the increase of the viscosity of the dispersed phase during the chemical reaction, the balance between the mechanism of coalescence and breakup was shifted to the coalescence process and led to larger particles. They showed that for a gel fraction of the dispersed phase higher than 0.4, the mechanism of coalescence and breakup was no longer suitable and that it was more realistic to speak about a coagulation process.

Actually, almost all of the experimental work on TP/TS polymer blend structure is focused on factors that control the final morphologies. Very few authors have tried to follow the development of the morphology from the beginning of the phase separation to the complete demixed system. Moreover, the aim of this work is to compare the morphologies obtained under static and shear conditions.

2. Experimental

2.1. Materials

The epoxy system consisted of a diglycidyl ether of bisphenol A (DGEBA) with a degree of polymerization of $n = 0.15$ cured with 4,4′-methylenebis(2,6-diethylaniline) (MDEA). This system has already been described elsewhere [33]. The thermoplastic (TP) polymer used in this study was an amorphous polystyrene, PS supplied by Atofina. The chemical structure and characteristics of the reactants are listed in Table 1.

2.2. Blend composition and preparation

The blend was composed of PS/DGEBA-MDEA (60/40). It was prepared in an internal Haake mixer (Polylab with 540P mixing chamber) using two non-reactive pre-extruded blends whose compositions were adjusted to obtain a stoichiometric mixture of epoxy with the amine comonomer (r = NH/epoxy = 1). The composition of the pre-blends

Table 1
Characteristics of the thermoplastic and the different reactants used

Products	Formula	M_n (g mol^{-1})	M_w (g mol^{-1})	T_g (°C)
Diglycidyl ether of bisphenol A DGEBA $\bar{n} = 0.15$ (Interdesco)	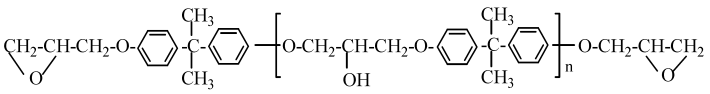	382.6		−27
4,4′Methylenebis (2,6-diethylaniline) MDEA (Lonza)	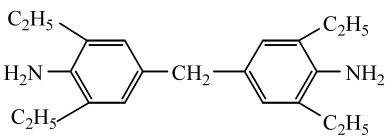	310.5		
Lacqrene PS 1450N (Atofina)	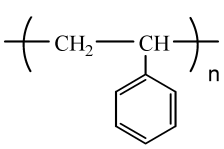	163 000	325 000	100

were the following: PS/DGEBA (50/50) and PS/MDEA (73.2/26.8).

To follow the evolution of the blend under shear, all the reaction proceeded into the mixer. The blending of the PS with the reactive system was performed at an average temperature of the molten blend of 177 °C and at 60 rpm in the 70 cm^3 mixing chamber equipped with the standard rotors. Fiftyfive grams of the pre-extruded blends were fed in the chamber. At selected time intervals, small samples were taken from the mixer chamber after the rotors were stopped; sampling time was about 5–10 s. A 1.5–2.5 g sample of polymer melt was removed with care being taken not to elongate or orient the sample to avoid altering the blend morphology. The sample was immediately quenched in an ice water bath.

For the static experiment, the rotors were stopped after 7 min of mixing and all the material was removed from the chamber. The reaction was then continued in a thermoregulated oil bath at 177 °C without stirring and samples were removed from the bath at selected time intervals. As before, the samples were quenched in iced water.

2.3. Techniques

Differential scanning calorimetry (DSC) analyses were conducted using a Mettler TA3000 apparatus under an argon atmosphere. Dynamic runs at constant heating rates were made in order to measure the glass transition temperature, T_g (onset value), and the epoxy-amine conversion of the thermoplastic/thermoset blend. The experiments were carried out in a temperature range from −100 to 350 °C at a heating rate of 10 °C/min. The conversion of epoxy groups, x, at time t, is given by $x = 1 - \Delta H(t)/\Delta H_0$ where ΔH_0 is the enthalpy of the reaction of the initial monomer mixture and $\Delta H(t)$ is the complementary enthalpy measured for a partially converted system on time t.

The gelation time obtained by dissolving the samples in tetrahydrofuran (THF) was considered to be the time at which the presence of an insoluble fraction was first observed.

After dissolution of the samples in tetrahydrofuran (THF), a centrifugation process was employed to separate the non-soluble thermosetting epoxy from the PS matrix and so to determine the insoluble fraction of epoxy growing network. After four centrifugations, the crosslinked phase was dried under vacuum until its mass remained constant. The insoluble fraction, f, is defined as the ratio between the mass of solid phase collected after the centrifugation, m, and the initial mass of epoxy-amine m_0; $f = m/m_0$.

The cloud point time was determined with a light transmission device [34], a technique which begins to detect particles when their average diameters are of the order of 0.1 μm.

The morphology of the blends was studied by scanning electron microscopy (SEM) using a Philips XL 20, by confocal microscopy (Carl Zeiss laser He–Ne and Ar) and by transmission electron microscopy (TEM) using a Philips CM 120. In the first case, fractured surfaces were prepared by cryogenic fracture. For TEM, samples were ultramicrotomed at room temperature and, subsequently, vapour stained using rutheniumtetroxide (RuO_4). TEM imaging was done on the microscope operating at 80 kV accelerating voltage. The apparent particle diameter was determined by numerizing TEM photomicrographs. Since the microtome does not necessarily cut the sphere at the largest section, a correction was applied, for the quiescent blend in order to obtain the actual diameter. The effective average particle diameter $d = (4 \times d_{measured})/\pi$ was calculated from an analysis of 100–400 particles taken from several TEM photomicrographs. The main uncertainty comes from the numerizing procedure. The surface fraction of dispersed phase S_d was calculated as $S_d = (\Sigma nA)/A_T$ where n is the number of particles having a diameter of d, A the area of particles and A_T the area of micrograph under analysis. The concentration of dispersed particles P is given as $P = (\Sigma n)/A_T$.

3. Results and discussion

3.1. Epoxy-amine reactions in 60% wt PS based blends

The conversion was measured for the quiescent and the dynamic system as a function of time (Fig. 2).

Before phase separation, the presence of the thermoplastic leads to a dilution of the reactive epoxy-amine functions. Consequently, the kinetics of the reactions are slower than those observed in bulk [14,35]. Upon phase separation, in our case after 22 min of reaction at 177 °C, dispersed droplets of epoxy-amine were formed which grew in size and number. Two phases coexist: an epoxy rich

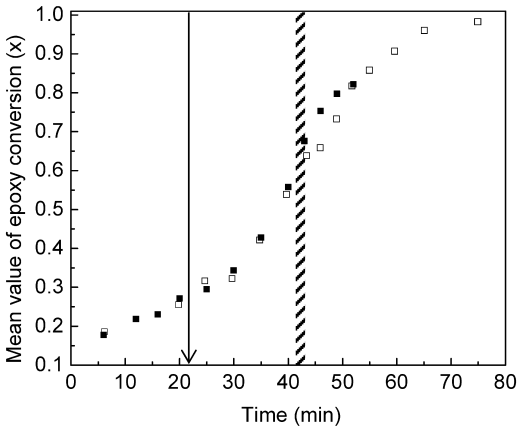

Fig. 2. Mean value of epoxy conversion (x) versus time for the static (■) and the dynamic (□) PS/DGEBA-MDEA (60/40) blends at 177 °C. Epoxy conversion is measured by DSC. The arrow ↓ indicates the cloud point. Gelation is also indicated (𝒻).

phase (α phase) and a PS rich phase (β phase). During this step, the dilution ratios change rapidly and differently in the α phase and the β phase. In fact, the epoxy conversion measured is a global value that integrates the epoxy conversion in both phases. The important result in our experiments is that the evolution of the mean value of epoxy conversion versus time for the static and the dynamic experiments is the same.

For the dynamic experiment, the superposition of the evolution of the mean value of epoxy conversion with the torque exerted on the rotors versus time (Fig. 3) is interesting since we have noted that the first appearance of insolubles corresponds to the sudden rise of the torque. We have also plotted the insoluble fraction of growing thermoset versus time in the same figure.

The rise of the torque matches the rise of the insoluble fraction. The gel fraction increased rapidly between 43 and 50 min which corresponds, respectively, to 0.20 and 0.75 and to an evolution of torque from 0.05 to 5 N m.

3.2. Phase compositions

One way to determine the composition of the phases of the blend is to measure the T_g of each phase. The evolution of the glass transition temperature (T_g) of the blend PS/DGEBA-MDEA (60/40) as a function of the epoxy-amine conversion is shown in Fig. 4. Before any discussion concerning the results, it is important to note that the processing temperature was always higher than the T_g of the two neat components so that no vitrification of any phase occurred.

The evolution of the T_g with time and conversion for the static and dynamic experiments is the same. When the mixture was homogeneous, only one T_g was observed. The phase separation is dominated by a nucleation and growth mechanism since the theoretical critical composition, ϕ_{crit} for the PS/DGEBA-MDEA (60/40) blend is 5 wt%. However after the phase separation, two T_gs were measured [14]. The upper one, $T_g(\beta)$, was attributed to the PS rich phase while the lower one, $T_g(\alpha)$, was attributed to the epoxy-amine rich phase. Both had different evolutions with curing time.

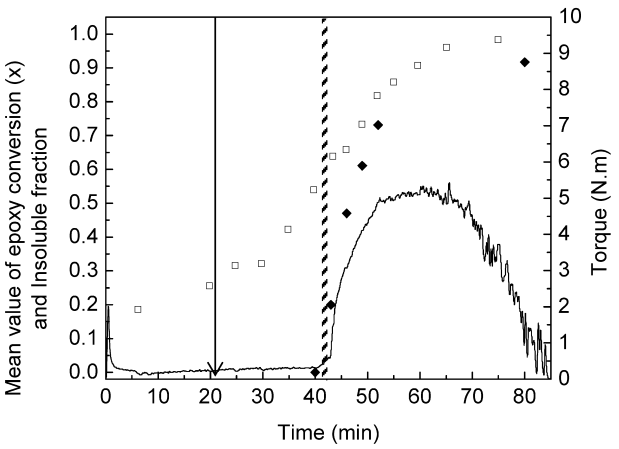

Fig. 3. Dynamic PS/DGEBA-MDEA (60/40) blend at 177 °C and 60 rpm into the mixer. Evolution of the global epoxy conversion (□), of the insoluble fraction (◆) and of the torque exerted on the rotors (-). The arrow indicates the cloud point. Gelation is also indicated (▨).

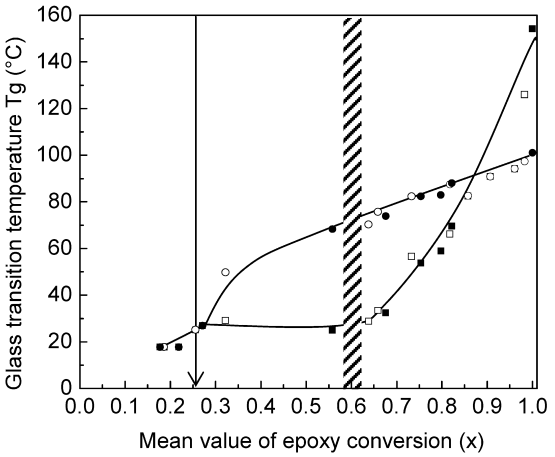

Fig. 4. Glass transition temperature T_g evolution versus the epoxy conversion for the static (■,●) and the dynamic (□,○) PS/DGEBA-MDEA (60/40) blend at 177 °C. (■,□) epoxy-amine rich phase, (●,○) polystyrene rich phase. Epoxy conversion and T_g were measured by DSC. The arrow ↓ indicates the cloud point x_{cp}. Gelation is also indicated (▨).

The glass transition temperature of the thermoplastic rich phase, $T_g(\beta)$ increases because of the rise of the concentration of the thermoplastic and the decrease of the concentration of monomers, dimers, etc in the β phase. At the end of the reaction $T_g(\beta) = T_g(PS)$, which means that the β phase is pure PS.

The evolution of the T_g of the dispersed phase, $T_g(\alpha)$ is more complex. On the one hand, the epoxy-amine particles are continuously fed by epoxy and amine i-mers coming from the β phase. This process tends to decrease the T_g of the dispersed phase. On the other hand, the epoxy-amine reaction in the particles increases the T_g. This explains why $T_g(\alpha)$ was relatively constant

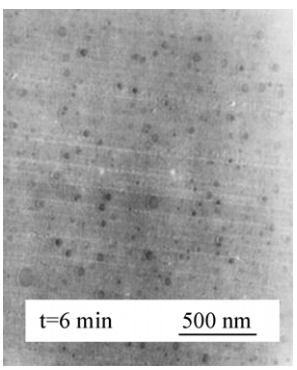

Fig. 5. Transmission electron micrograph of the PS/DGEBA-MDEA (60/40) blend after 6 min of shearing at 177 °C and a quench at 0 °C.

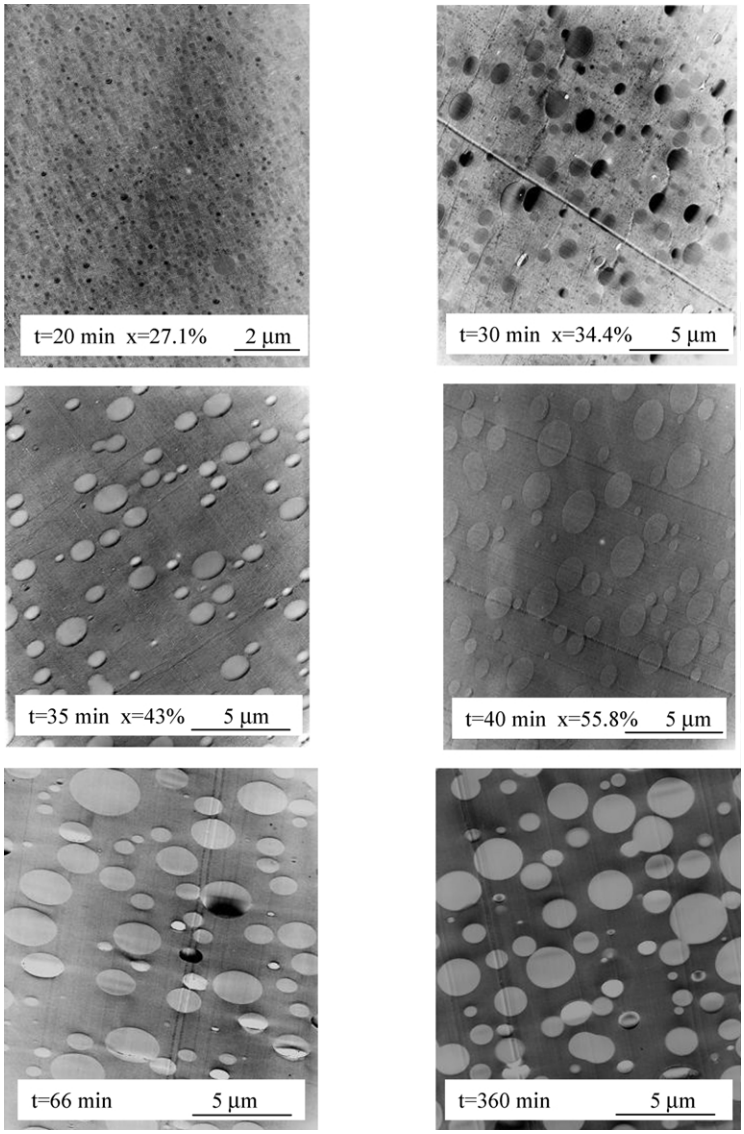

Fig. 6. Transmission electron micrographs of the PS/DGEBA-MDEA (60/40) system at different stages of phase separation induced by polymerization at 177 °C in quiescent conditions. The characteristics of the systems are $x_{cp} = 0.27$; $0.56 < x_{gel} < 0.63$.

before increasing after $x = 0.64$. At the end of the reaction, $T_g(\alpha)$ is equal to the T_g of a neat DGEBA-MDEA network. In the region of the gelation of the dispersed phase, the T_g of the PS is 70 °C, which means that this phase is still purifying since the T_g of neat polystyrene is only reached at the end of the reaction. Until the end of the epoxy-amine reaction, epoxy-amine oligomers migrate from the continuous phase. This phenomenon is not influenced by the static or dynamic nature of the process.

The global epoxy conversion and the glass transition temperature of the phases are the same for the quiescent and the dynamic systems. Thus the evolution of reaction and phase compositions for static and dynamic blends are the same that means that they are not controlled by diffusion processes. This is an important first conclusion from our experiments.

3.3. Evolution of morphologies of the PS/DGEBA-MDEA (60/40) blend in quiescent conditions

Before analysing the results, it must be kept in mind that all the microscopic analyses were performed at room temperature after a rapid thermal quench from 177 °C to room temperature. Fig. 5 shows that, in these experimental conditions, dispersed domains of epoxy-amine with size ranging from 10 to 100 nm exist before the time at which phase separation occurs identified by the cloud point measurement.

The diameter of these particles is much smaller (50 nm) than the one of the particles produced by the polymerisation induced phase separation (500 nm) at the beginning of the phase separation) so they were attributed to a thermal induced phase separation during the thermal quenching of the sample. After this observation it was assumed that the

effect of thermal quench on observed morphologies was negligible. Fig. 6 shows the evolution of the morphology observed by TEM of the blend PS/DGEBA-MDEA (60/40) under quiescent conditions at 177 °C. Blends containing 60 wt% PS exhibited morphologies consisting of a dispersion of spherical thermoset-rich particles in a thermoplastic matrix. The shape remains spherical during all the entire process.

The dispersed phase average particle size, the surface fraction and the concentration of the dispersed phase particles are plotted as a function of time in Fig. 7.

The particles grow during the period from 20 to 55 min, then their growth rate decreases leading to a final diameter of 2.8 μm. Fig. 7 shows that the morphology continues to evolve even when the gel point of the dispersed phase is overtaken. The surface fraction increases indicating both the growth of particles and/or the appearance of new particles.

Concurrently, the concentration of the dispersed phase rises until nearly the gel point indicating that some particles are new nucleated, then it decreases showing some coalescence. The change in size can be explained by (a) the diffusion of the i-mers from the TP rich matrix towards epoxy/amine rich dispersed particles and (b) coalescence of the dispersed phase and/or the evaporation–condensation process. However, it is difficult, in such systems, to discriminate between coalescence and evaporation/condensation. It can be argued that evaporation–condensation is not going to dominate because of the increase of the viscosity of our system and of the fraction of the dispersed phase which leads to a decrease of the distance between two particles. Finally, the particles have a mean diameter of 2.8 μm. Fig. 8 illustrates the fusion of two particles of epoxy/amine.

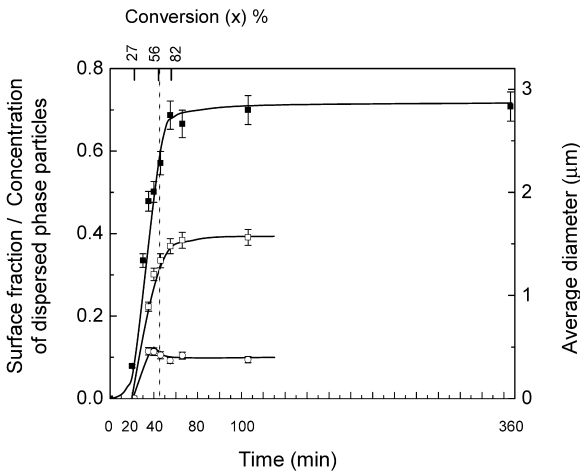

Fig. 7. Average dispersed phase particle size (■), surface fraction of dispersed phase(□) and concentration of dispersed phase (○) for PS/DGEBA-MDEA (60/40) blend as a function of reaction time in static conditions. The characteristics of the systems are: $t_{cp} = 22$ min, $40 < t_{gel} \leq 43$ min. (▨) Gelation region.

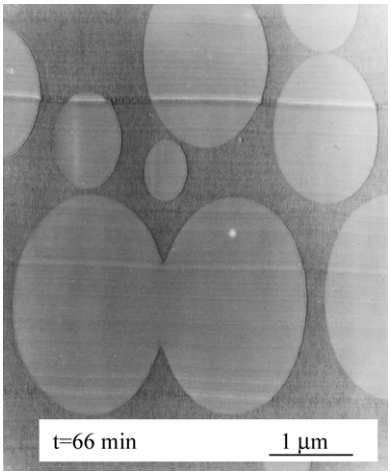

Fig. 8. Illustration of the fusion of two particles of epoxy-amine in quiescent condition at $t = 66$ min and $x \sim 0.9$.

3.4. Evolution of the morphologies of the PS/DGEBA-MDEA (60/40) blend in dynamic conditions

As was done for the quiescent study, we represent the evolution of the morphology of the blend PS/DGEBA-MDEA (60/40) under dynamic conditions at 177 °C in Fig. 9. Quantitative analysis of the morphologies of Fig. 9 for different reaction times is shown in Fig. 10. Because of the irregular shapes of particles, we have measured the area of the particles. In Fig. 10, the X-axis represents a class of particle area named a. On the Y-axis, A is the normalized particle area defined as the product of a and f (the frequency of the occurrence of a.

During the first 35 min of mixing (Fig. 10a and b), the morphology of the blend consists of a dispersion of spherical epoxy-rich particles. The area of the particles does not exceed 2 μm^2 until 30 min of shearing. As far as the dispersed particles are viewed as a viscous liquid (before the gel point), the mechanism of coalescence and break-up is possible as in classical thermoplastic/thermoplastic blends. Thus the shape of the particles remains spherical because the process of shape relaxation is possible (see Fig. 9). Compared to the size of the particles under static conditions, those obtained under shear are smaller indicating that the break up process occurs and that it is more important than the coalescence process.

Around 43 min (Fig. 10c), the time for epoxy gelation, the particle area distribution broadens significantly leading to a bimodal particle size distribution consisting of small spherical particles of 0.8–1 μm ($a < 2\ \mu m^2$) and large, irregular particles of 10 μm ($2 < a < 24 \mu m^2$) (see Fig. 10). The first population with small size (Fig. 10c) is composed of newly nucleated particles that have nucleated in a very viscous matrix. We assume that these small particles are formed continuously until the gelation of the dispersed phase rather than formed by the tipstreaming process. These small particles coalesce preferentially and rapidly because the time to drain the film is shorter for small particles. To

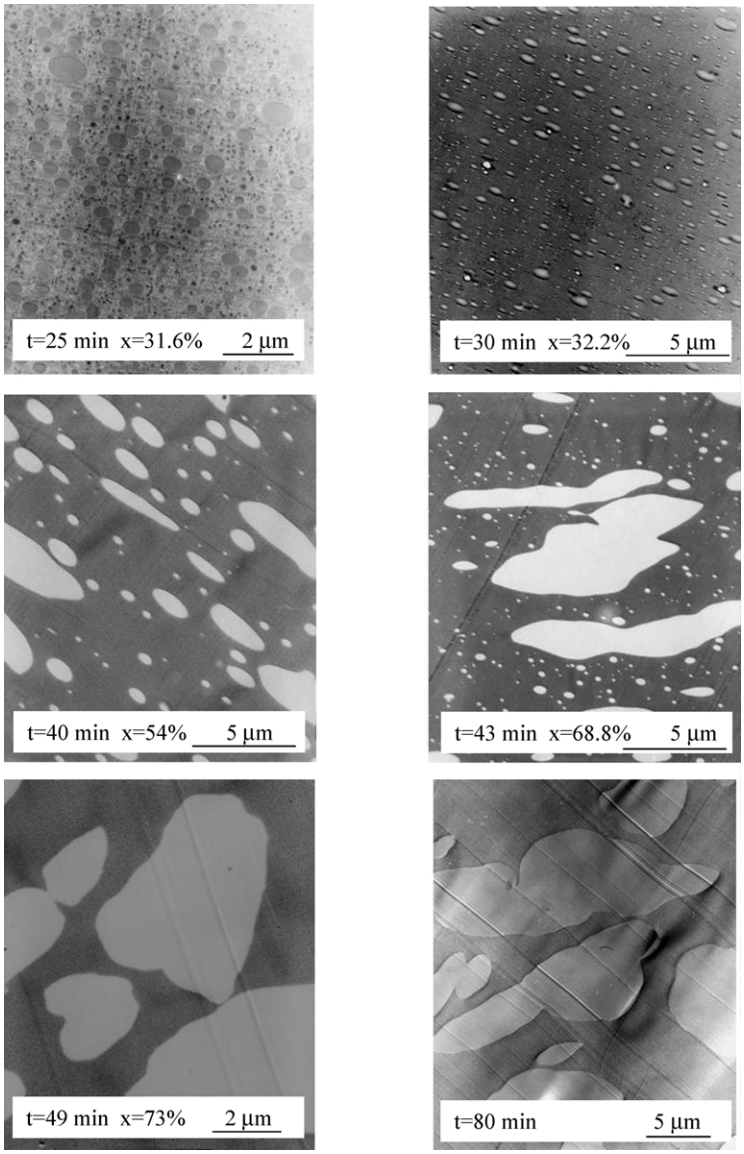

Fig. 9. Transmission electron micrographs of the PS/DGEBA-MDEA (60/40) system at different stages of phase separation induced by polymerization at 177 °C in dynamic conditions. The characteristics of the systems are $x_{cp} = 0.27$; $0.56 < x_{gel} < 0.63$.

ensure a certain collision frequency, we raised the speed of the rotors before the gel point. Once again, the bimodal particle size distribution was present after the gelation time.

The large particles are the result of the coalescence of small and spherical particles formed during the first step of the process. Moreover with the chemical reaction, the viscosities of the dispersed phase increases rapidly. Due to the development of the elasticity of the crosslinked particles plus the shearing and taking into account the fact that the crosslinked droplets are reactive so that covalent bonds at the interface may be created, the relaxation of shape normally leading to spherical particles and the breakup process become impossible. In that case, it is more realistic to speak about a reactive agglomeration than a coalescence process.

Fig. 11 illustrates the reactive agglomeration process during shearing of a reactive blend after the crosslinking of the dispersed phase.

In 6 min of shearing the smaller particles of the bimodal distribution disappear totally since after 49 min of reaction (Fig. 10e) in the mixer, no particles smaller than 2 μm^2 are observed.

Finally, at the end of the process, only large and irregular particles of about 10 µm are present in the blend under shear. The scanning electron microscopy is also interesting because it offers a better view of the topography of the blend and the three-dimensional image obtained by confocal microscopy (Fig. 12a) clearly shows the irregular and large shape of the epoxy-amine nodules obtained under shear at the end of the reaction.

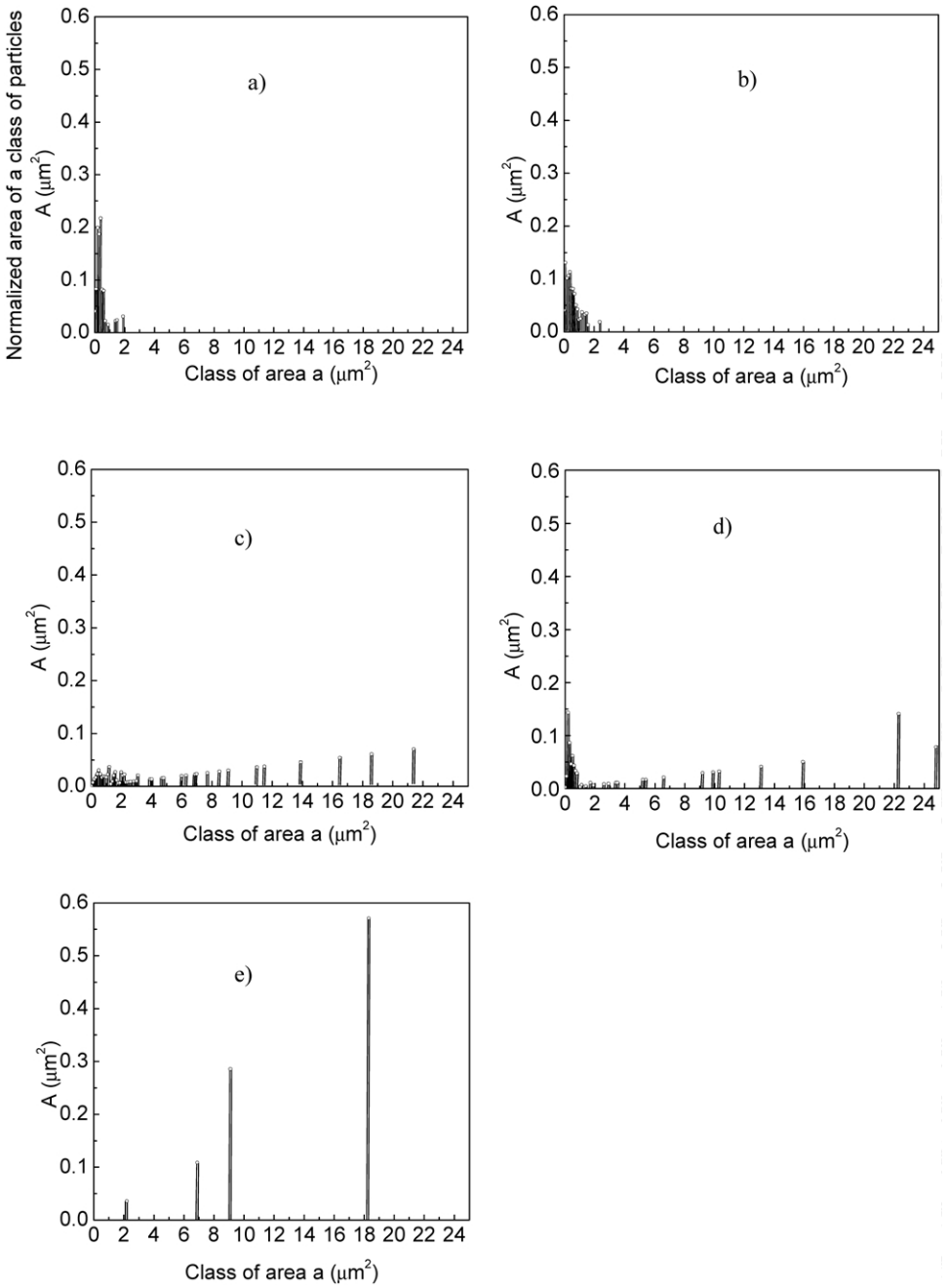

Fig. 10. Particles area (μm^2) distribution for PS/DGEBA-MDEA (60/40) at 60 rpm and 177 °C. (a) $t = 25$ min, (b) $t = 30$ min, (c) $t = 40$ min, (d) $t = 43$ min, (e) $t = 49$ min.

De Loor et al. [32] have shown, in the case of an EVA/EMA network, the existence of a critical gel fraction equal to 0.4 from which the coalescence and break-up mechanism is prevented. In our blend, the classical mechanism of coalescence and break-up cannot be applied after the gel point and for a gel fraction value between 0.2 and 0.46 (Figs. 3 and 9).

Fig. 13 summarizes the mechanism of the morphology development of an initially miscible TP/TS blend under shear.

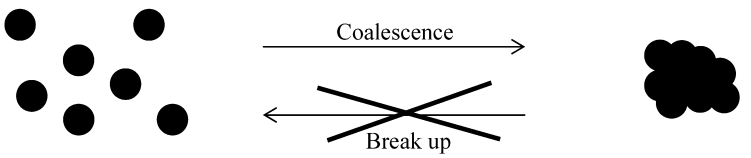

Fig. 11. Schematic illustration of the 'reactive agglomeration' process of a reactive blend under shear.

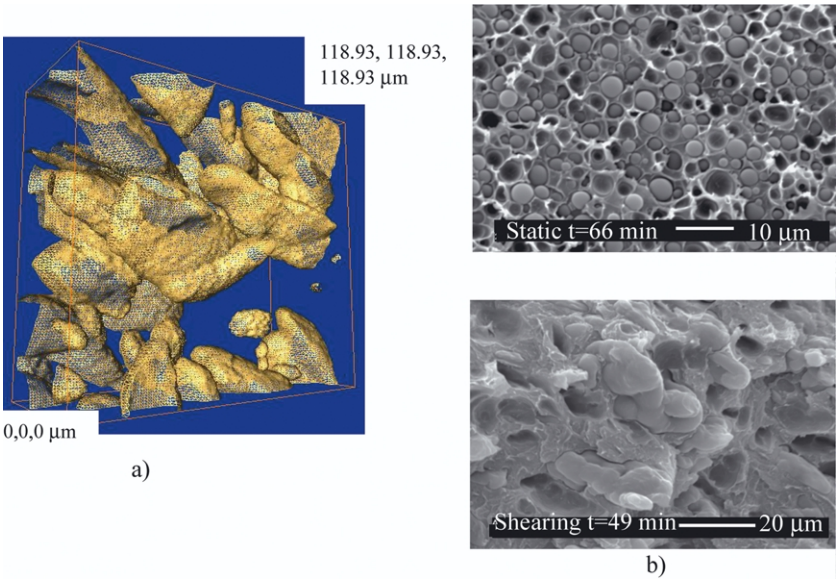

Fig. 12. (a) Confocal micrograph of the DGEBA-MDEA particles obtained at the end of reaction at 177 °C under dynamic conditions. (b) Comparison between scanning electron micrographs obtained under static and dynamic conditions.

4. Conclusion

Because the size and the shape of the dispersed phase can influence mechanical or other properties, our aim was to clearly understand the mechanisms of morphology development and the way it takes place under shear for a model system.

With this model, we have shown that the way the reaction induced phase separation process takes place either under static conditions (without flow) or under shear, does not affect the mean value of epoxy conversion and the glass transition temperatures. Thus the evolution of phase compositions for static and dynamic blends are the same and do not influence the morphologies evolutions. However, the final size and shape of the particles strongly depends on the process: the final morphology of the PS/DGEBA-MDEA (60/40) blend consists, under quiescent conditions, of a dispersion of spherical thermoset rich particles of 2.8 µm; under shear, the particles are no more spherical when the gel point is reached and irregular particles of 10 µm characterize the final morphology.

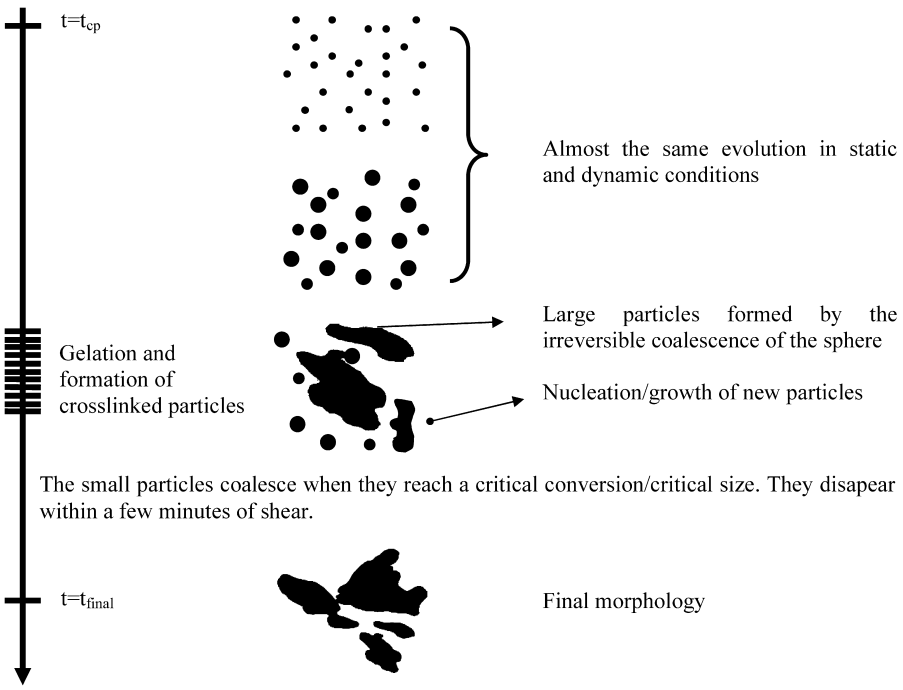

Fig. 13. Process of development of particles under shear for a reactive blend.

In the quiescent situation, the evolution of the morphology can be explained by physical phenomena such as the fusion of neighbouring droplets and/or evaporation–condensation.

Under shear, the relaxation of shape leading to spherical particles becomes impossible because of the formation of covalent bonds and due to the increased of elasticity of the dispersed phase. We have shown that the classical break-up/coalescence behaviour, generally observed for thermoplastic/thermoplastic blends subjected to flow, is valid only before the gel point. It appears that the morphologies are strongly dependant, not only on the evolution of the viscosity ratio between the matrix and the dispersed phase, but also on the gel point and the crosslinking phenomena of the dispersed phase.

Acknowledgements

The authors are indebted to Professor Bernango of the Centre commun de quantimétrie et d'analyse de la faculté de Médecine et de Pharmacie de Lyon for his help in confocal microscopy and in the TEM image analysis.

References

[1] Pascault JP, Williams RJJ, Polymer blends, vol. 1. New York: Wiley-Interscience; 2000. p. 379.
[2] Girard-Reydet E, Sautereau H, Pascault JP, Keates P, Navard P, Thollet G, Vigier G. Polymer 1998;39:2269.
[3] Favis BD, Chalifoux JP. Polymer 1988;29:1761.
[4] Elmendorp JJ, Van Der Vegt AK. Polym Engng Sci 1986;26:1332.
[5] Sundararaj U, Macosoko CW. Macromolecules 1995;28:2647.
[6] Gonzalez-Nunez R, De Kee D, Favis BD. Polymer 1996;37:4689.
[7] Potente H, Bastian M, Gehring A, Stephan M, Potschke PJ. Appl Polym Sci 2000;76(5):708.
[8] Williams RJJ, Rozenberg BA, Pascault JP. Adv Polym Sci 1997;128:95.
[9] Grace HP. Chem Engng Commun 1982;14:225.
[10] Wu S. Polym Engng Sci 1987;27:335.
[11] Wildes G, Keskkula H, Paul DR. J Polym Sci, Polym Phys 1999;37:71.
[12] Chapleau N, Favis BD, Carreau. J Polym Sci, Polym Phys 1998;36:1947.
[13] Willis JM, Caldas V, Favis BD. J Mater. Sci. 1991;26:4742.
[14] Bonnet A, Pascault JP, Sautereau H, Taha M. Macromolecules 1999;32:8517.
[15] Venderbosch RW, Meijer HEH, Lemstra PJ. Polymer 1994;33(20):4349.
[16] Venderbosch RW, Meijer HEH, Lemstra PJ. Polymer 1995;36(6):1167.
[17] Venderbosch RW, Meijer HEH, Lemstra PJ. Polymer 1995;36(15):2903.
[18] Jansen BJP, Meijer HEH, Lemstra PJ. Polymer 1999;40:2917.
[19] Fortelny I, Zivny A, Juza. J Polym Sci, Polym Phys 1999;37:181.
[20] Crist B, Nesarikar AR. Macromolecules 1995;28:890.
[21] Elmendorp JJ, Van Der Vegt AK. Polym Engng Sci 1986;26:1332.
[22] Saboni A, Gourdon C, Chesters AK. J Colloid Interf Sci 1995;175(1):27.
[23] Smoluchowski MM. Phys Z 1916;17(557):585.
[24] Tanaka H. Phys Rev Lett 1994;72(11):1702.
[25] Lifshitz IM, Slyozov VVJ. Phys Chem Solids 1961;19:35.
[26] Voorhees PW. J Stat Phys 1985;38:231.
[27] Mirabella FM, Barley JS. J Polym Sci, Polym Phys 1994;32:2187.
[28] Taylor GI. Proc Roy Soc, London A 1932;138:41.
[29] Taylor GI. Proc Roy Soc, London A 1934;146:501.
[30] Janssen JMH. The dynamics of liquid–liquid mixing : a review, in materials science and technology : a comprehensive treatment, processing of polymers; 1997; 18:113.
[31] Vivier T. PhD, 96 STR1 3164.
[32] De Loor A, Cassagnau P, Michel A, Vergnes B. J Appl Polym Sci 1994;53(12):1675.
[33] Eloundou JP, Ayina O, Ntede Nga H, Gerard JF, Pascault JP, Boiteux G, Seytre G. J Polym Sci, Polym Phys 1998;36:2911.
[34] Moschiar SM, Riccardi CC, Williams RJJ, Verchere D, Sautereau H, Pascault JP. J Appl Polym Sci 1991;42(3):717.
[35] Swier S, Van Mele B. Thermochim Acta 1999;330:175.